Modeling and Simulation of a Micro pump and Its Performance
نمذجة ومحاكاة مضخة دقيقة وادائها

Mohamed R. Ibrahim, Mohamed H. Mansour and Mohamed Nabil Sabry

Mechanical Power Engineering Department, Faculty of Engineering,
Mansoura University, El-Mansoura 35516, Egypt
Emails: the_best3830@yahoo.com, mhsaadanym@mans.edu.eg, mnabil.sabry@gmail.com

الخلاصة

تم عمل نموذج للسريان غير المستقر ثنائي الأبعاد لمحاكاة مضخة دقيقة بدون صمامات واستخدامه لدراسة أداء المضخة في مختلف ظروف التشغيل. تم دراسة أثر ظروف التشغيل ومعاملات التصميم وخواص المائع على أداء المضخة. تبين أن تردد التشغيل له أثر حاسم وأن هناك تردد رنين ينتج عنه أعلى معدل سريان. تم التركيز على دراسة باقي العوامل على تردد الرنين. كما تم أيضا استنباط علاقات غير بعدية للتنبؤ بأداء المضخة بدرجة دقة كافية وذلك في إطار حيز الدراسة.

Abstract

A transient 2D model of Valve-less micro-pump is constructed and used to study pump performance under different conditions through numerical simulation. Operating conditions, design parameters and fluid properties effect on the micro pump net flow rate have been investigated. The operating frequency was found to be a critical operating parameter. Therefore, the effect of other design and operating conditions on the resonance frequency (optimum operating frequency) has been studied. Also, general correlations for the micro pump dimensionless performance characteristics have been deduced with sufficient accuracy, within the studied range.

Keywords

1   Introduction

Micro pumps were widely used during the few last decades. Regardless of the actuation method used, valve-less micro pumps have many advantages. For example, no blocking may occur during valve movement due to the presence of impurities for instance. In addition, the reduction of mechanical moving parts allows long life span. It is used in a huge number of fields and applications such as medical, chemical, biological and engineering fields. Furthermore, it represents the main part of many systems (drug delivery systems, Lab-on-a-chip, inkjets, etc.), Abhari et al. (2012). Valve-less micro pumps consist of a moving membrane (i.e. diaphragm), micro pump chamber and rectification elements at inlet and outlet. A rectification element allows more flow to pass in one direction than flow in the opposite direction. Conventional rectification elements used are nozzle/diffuser elements. Rectification elements used for this work are abrupt contraction/expansion elements. Figure 1 shows the main parts of the studied micro pump. When a sinusoidal actuation force is applied to the diaphragm, there are two strokes. The first one is suction stroke, which happens when the diaphragm is deflected upwards. Hence, the fluid flows into the pump through inlet and outlet. The inlet section acts as an abrupt expansion element while the outlet element acts as abrupt contraction. As will be shown in this work, at low frequencies, the flow rate through inlet is higher than through outlet.
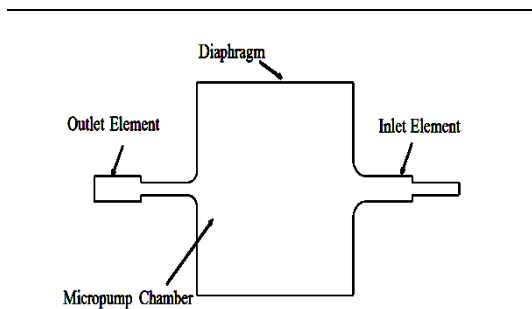
Figure 1 Micro pump main components

The second stroke is a discharge stroke, which occurs when the diaphragm is deflected downwards. The flow is then forced to flow outside the pump, and the inlet section acts as an abrupt contraction while the outlet section acts as an abrupt expansion. In this case, the amount of flow rate through the inlet is lower than that through outlet during the discharge stroke. This difference in flow rate through the two operating strokes produces a net flow rate through the outlet section. The direction of net flow may change according to operating and design conditions, as will be proved in this work.

During the few last decades, the number of publications about micro pumps has been increased due to their great importance for most modern applications. Li and Chen (2003) presented an analytical analysis of a circular Lead Zirconate Titanate (PZT) actuator. They verified their simulation results with an analytical analysis of the actuator. They concluded that using their simulation results can help in selecting and optimizing the actuator before fabrication. However, their analysis was limited to low frequencies. Singhal et al. (2004) presented a comprehensive study on diffuser/nozzle elements used in a valve-less micro pump. They examined four types of diffusers and studied the effect of Reynolds number variation and the inclination angle of the diffuser on the pressure loss across it. They concluded that the flow rectification

also occurs in laminar flow. Furthermore, Fan et al. (2005) studied the performance of piezoelectric actuated valve-less micro pump considering electro-mechanical-fluid coupling. In their study, the main parameter was the actuation frequency. The results of simulation indicated that the optimal actuating frequency for the micro pump is achieved at a lower frequency than the first nature frequency. Nagy (2005) studied the effect of operating frequency on two types of micro pumps. He obtained the same previous result of Fan et al. (2005). Ahmadian and Mehrabian (2006) presented a design optimization by studying the operating and design parameters on the micro pump net flow rate. Based on the simulation results, they presented a correlation between the optimized diffuser angle and the actuation pressure. The effect of operating frequency is not studied. Also, a three dimensional (3D) simulation has been presented by Lan et al. (2008) for the solid-fluid coupling of valve-less micro pump. They reported that the pump flow rate mainly depends on operating frequency. Optimum frequency depends on the piezoelectric plate size. Moreover, regarding micro pump design, Yang et al. (2008) described the design and fabrication process of peristaltic (i.e. series connection) micro pump with three membranes. They reported that the wriggling transportation of fluid is very smooth and supply high flow rate. Johari and Majlis (2010) studied numerically the piezoelectric actuated valve-less micro pump. They found that micro pump performance not only depends on the operating frequency, but also on the deflection shape of the membrane. Also, Devarajan et al. (2011) studied the micro pump performance at steady state. They introduced a steady suction and steady discharge strokes and suggested that it is better to find a suitable method for modeling the moving wall diaphragm. Yang et al. (2011) studied experimentally and

numerically the effect of operating frequency on net flow rate. They found that the net flow rate increases with increasing frequency until it reaches its maximum value, then decreases with any further increase in frequency. They also studied the back pressure effect on the micro pump performance. They reported that increasing back pressure always decreases net flow rate. Singh et al. (2015) presented an analytical, numerical and experimental study for planer valve-less micro pump with a limited range (very low) of operating frequencies. They found that the micro pump net flow rate is depending on various parameters including amplitude and frequency of the actuation force, membrane material, thickness and diameter, diffuser/nozzle inlet and throat areas. They reported that the maximum flow rate occurs at the natural frequency, which have a strong dependence on the mass of liquid within the diffuser/nozzle elements and within the micro pump chamber.

From the previous review, it is found that all types of valve-less micro pump have been modeled and fabricated in the same shape, in which inlet and outlet rectification elements are diffuser/nozzle elements. To the authors' knowledge, no other types of rectification sections have been studied. Moreover, no comprehensive study of micro pump design and its operating parameters are yet available. As it is a very complicated work to be completely studied, most researches were performed to understand the effect of one or two of its operating parameters and design conditions.

The objective of this study is to understand problem physics in order to deduce the effect of operating parameters and design conditions on micro pump performance, on a clear basis. The study uses abrupt expansion/contraction elements for rectification process rather than diffuser/nozzle elements, which are significantly simpler to be fabricated.

2   Model description
2.1   List of assumptions
- Incompressible fluid
- Newtonian fluid
- Isothermal
- Very small dimensions (microscale)
- Laminar flow
- Very smooth walls

2.2   Governing equations
Based on the listed assumptions, mass and momentum conservation equations can be written as the following:

$$\nabla . V = 0 \tag{1}$$

$$\rho \left[\frac{\partial V}{\partial t} + (V . \nabla V) \right] = -\nabla p + \mu \nabla^2 V \tag{2}$$

2.3   Boundary conditions
Boundary conditions for all simulated cases are shown in Figure 2. The value of peak velocity, operating frequency and back pressure are changed for the different cases studied.
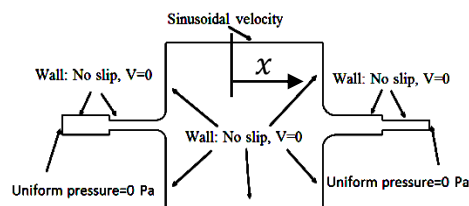
Figure 2 Micropump Boundary conditions

The applied inlet velocity, which is expressed by equation (Error! Reference source not found.), is programmed in C language and interpreted as (UDF) with ANSYS Fluent simulator.

$$V = V_o \, sin(\omega t) * (1 - \frac{4x^2}{D^2})$$

where
V Instantaneous velocity, m/s

V_o Peak velocity, m/s
ω Angular frequency, rad/s
t Time, s
x Horizontal distance from
       diaphragm center, m
D Diaphragm width, m

3 Mesh generation
3.1 Mesh generation

Gambit 2.3.16 was used to create and mesh the geometry. Once the meshing is completed, a mesh file is exported to ANSYS Fluent to solve the governing equations within the domain. Then, ANSYS CFD-Post is used for post processing task and analyzing the results. The model geometry was divided into three sections. The first section is the pump chamber, which has a quads algorithm mesh and mesh size of 3 µm/cell. While, the second part is the connection between pump chamber and abrupt expansion/contraction elements. It has a triangular algorithm of mesh size 2 µm/cell. The third part is the abrupt expansion/contraction elements. It has a quads algorithm and a mesh size of 1 µm /cell.

3.2 Solver

Computational Fluid Dynamics (CFD) simulations were utilized to analyze the two dimensional flow within micro pump. The flow is assumed to be laminar, isothermal, Newtonian and incompressible. The transient laminar flow model coupled was employed to simulate the flow field. The simulations have been performed using the computational fluid dynamics software called ANSYS Fluent 15.0. The SIMPLE algorithm was used to solve the pressure-velocity coupling.

4 Geometry of the main case

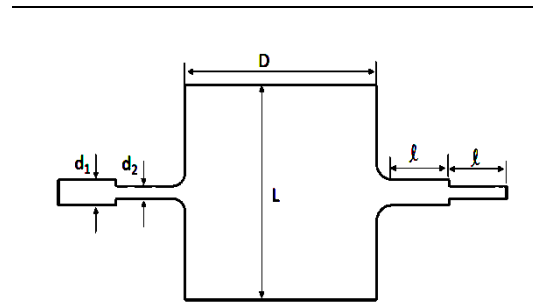The main case study and its design parameters are illustrated in Figure 3.

Figure 3 Micro pump design parameters

The diaphragm peak velocity, operating frequency and back pressure are 0.5 m/s, 4000Hz and 0 Pa, respectively. The design conditions are D=500 µm, L=500 µm, l=150 µm, d_1=60 µm and d_2=30 µm as shown in Figure 3. The depth of the micro pump is taken 1 mm and the velocity is assumed uniform in the depth direction. Hence, there are two area ratios, corresponding to these dimensions, AR_1= d_1/d_2=2 and AR_2=D/d_1=500/60. Finally, the fluid used was water, which has density (ρ) and dynamic viscosity (μ) of 998.2 kg/m^3 and 0.001 Pa.s, respectively. These values are kept constant for all simulation cases except the studied parameters.

5 Verification and validation
5.1 Verification

To perform a mesh independence study, some grid types and sizes were tested. Also, the solution should be examined with different time step sizes until an accepted error is reached. For this study, the selected peak velocity and operating frequency were 0.8 m/s and 5000 Hz, respectively. Also, the diaphragm width of 500 □m and abrupt area ratio of 2 were used.

5.1.1 Mesh dependency

In this regard, four cases were examined for mesh dependency. The details of the four cases are listed below in Table 1.

Table 1 Cases for mesh dependency

Cases	Mesh type	Cell size μm/cell
Case 1	Triangular algorithm	1.2
Case 2	Triangular algorithm	2
Case 3	Triangular algorithm	4
Case 4	The described case in section 3.1	

The net flow rate (Q_{net}) was compared for the previous cases. Table 2 shows the corresponding net flow rate and the relative error for each case.

Table 2 Net flow rate for examined mesh dependency cases

Case	Q_{net}, μL/min	% Error
Case 1	637	0
Case 2	653.9	2.64
Case 3	656.4	3.01
Case 4	639.2	0.34

Therefore, case 4 is selected for its accepted error and less running time.

5.1.2   Time discretization error

The time step size (Δt) was examined and checked for time discretization error because this study is performed for unsteady simulations. The used mesh is that selected from the mesh dependency study. The selected time steps are according to the corresponding number of time steps per cycle (n). Therefore, the time step can be calculated for any operating frequency (f) using the following equation:

$$\Delta t = \frac{1}{f * n} \qquad (4)$$

The examined cases applies peak velocity of 0.8 m/s and operating frequency of 5000 Hz and corresponding to the number of time steps per cycle of 10, 20, 50 and 100. The examined cases, the net flow rate and the corresponding relative error are listed in Table 3.

Table 3 Time discretization error cases

Case name	n	μt, s	Q_{net}, μL/min	% Error
Case 5	10	2e-5	619	3.88
Case 6	20	1e-5	631.1	1.99
Case 7	50	4e-6	639.2	0.709
Case 8	100	2e-6	644	0

Hence, the selected case is case 7 of number of time steps per cycle of (n=50), as it saves the running time and power and has an accepted error.

5.2   Validation

Validation task is divided into two steps. The first step is to validate only the effect of time change regardless of the area change. Hence, a pulsating flow within a straight duct is to be validated by comparing with the analytical solution as it will be discussed below. The second step is to validate the effect of area change, so the steady flow through an abrupt area change duct is to be validated. Hence, the whole effect is considered to be validated.

5.2.1   Pulsating flow through duct

The present work (i.e. numerical solution) is compared to the analytical solution presented by Yakhot et al. (1999). Figure 4 shows the difference between analytical and numerical solution at a certain time and frequency with a maximum relative error of 0.62%.
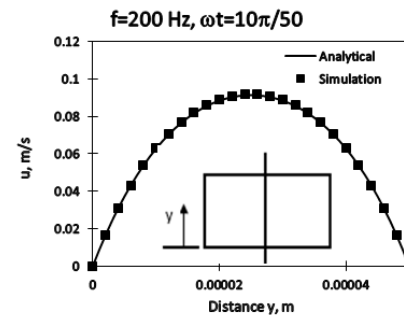
Figure 4 Analytical and numerical velocity distribution at frequency (f= 200 Hz) and time corresponding to ω t=10π/50

Hence, the first part is completely validated with the analytical solution.

5.2.2 Laminar steady flow through abrupt area change section

Ray et al. (2012) studied the laminar steady flow through the abrupt area change section (contraction) shown in Figure 5. Figure compares the numerical solution presented by Ray et al. (2012) and the present study solution for the same dimensions and boundary conditions. The maximum relative error was found to be about 4.3%.
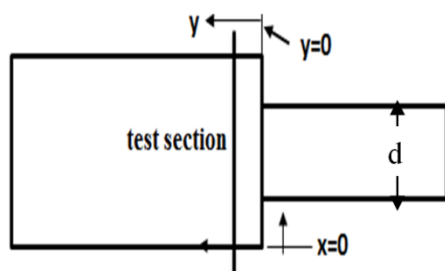

Figure 5 Test section

Then, the steady laminar flow through abrupt area change element (contraction) is validated. Hence, the whole case is considered to be validated.
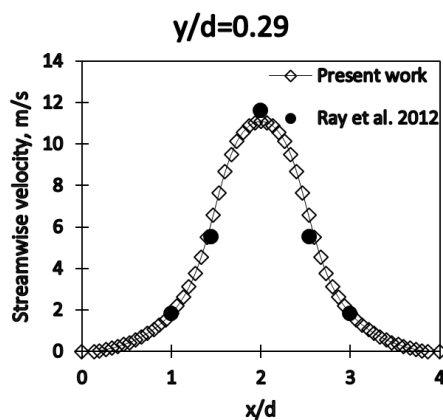

Figure 6 Comparison between (Ray et al. 2012) and present study numerical solutions

6   Results and discussion

The effects of various operating parameters, design conditions and fluid properties on micro pump performance were studied.

6.1   Net flow rate

In all simulated cases, the instantaneous flow rate has the same trend as shown in Figure 6. Flow rate through the inlet section is higher than that through the outlet section at the first half of the cycle (suction stroke). The process is reversed for the next half of the cycle (discharge stroke). This action is responsible for flow rectification through the micro pump. The same trend was obtained by Singh et al. (2015), regardless of the rectification elements shape.

6.2   Peak velocity and operating frequency effect

Figure 7 shows the effect of operating frequency at various peak velocity values on the micro pump net flow rate at zero back pressure.

As shown in thes figure, the net flow rate increases with increasing the peak velocity. Moreover, the net flow rate increases with increasing the operating frequency till it reaches its maximum value at resonance frequency. Then, it decreases with any further increase in operating frequency. The same trend for the frequency effect on the net flow rate was also obtained by Singh et al. (2015) and Herz et al. (2008).
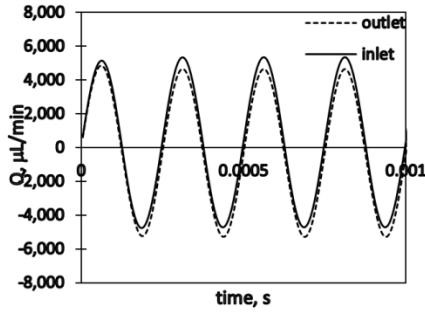
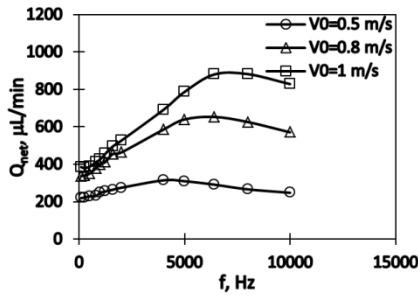*Figure 6 Instantaneous flow rate*

Figure 7 Operating frequency effect on the net flow rate at various peak velocities

Because the system exhibits resonance, the second order response of a linear system was used as a basis to select the correlation form. The one dimensional momentum balance for the pulsating flow through a straight duct gives the velocity ratio (ratio of the maximum produced velocity to the steady velocity) as the following, Rabie (2015);

$$\frac{V_a}{V_{st}} = \frac{C}{\sqrt{1 + (\tau.\omega)^2}}$$

Whereas the velocity ratio through the abrupt area change element is differs for both forward and backward directions to take the following form:

$$\frac{V_a}{V_{st}} = \frac{C_i}{\sqrt{1 + (\tau_i.\omega)^2}}$$

i=1 for forward direction and i=2 for backward direction

Then, the coefficients are differs for both directions and consequently produce a net flow rate in a certain direction as given below:

$$\frac{Q_{net}}{Q_0} = \frac{Q_{forward} - Q_{backward}}{Q_{ref}} =$$
$$AR * \left[\frac{V_a)_{forward}}{V_{st}} - \frac{V_a)_{backward}}{V_{st}} \right]$$

This net flow rate is also expected for the micro pump as given below:

$$\frac{Q_{net}}{Q_0} = \frac{\grave{C}_1}{\sqrt{1 + (\grave{\tau}_1\omega)^2}} - \frac{\grave{C}_2}{\sqrt{1 + (\grave{\tau}_2\omega)^2}}$$

This form is approximately takes the following form which fits the net flow rate for the micro pump:

$$Q_{net|p=0} \left(\frac{\mu L}{min} \right) = \frac{Q_0[1 + \left(\frac{f}{f_0} \right)]}{\sqrt{[1 - \left(\frac{f}{f_0} \right)^2]^2 + 4*\xi^2*\left(\frac{f}{f_0} \right)^2}} \quad (5)$$

Equation (Error! Reference source not found.) is applicable for the studied range of peak velocity and operating frequency using the following correlations.

$$f_0 = 5700e^{0.4V_0}$$

$$\xi = 1.26e^{-1.1V_0}$$

$$Q_0 = 240\ln(V_0) + 388$$

Applying these correlations to the case of peak velocity (V_0=1 m/s) and comparing the results with that obtained from the numerical simulation are depicted in Fig 8. These correlations have a maximum relative error of 9% for all simulation cases.
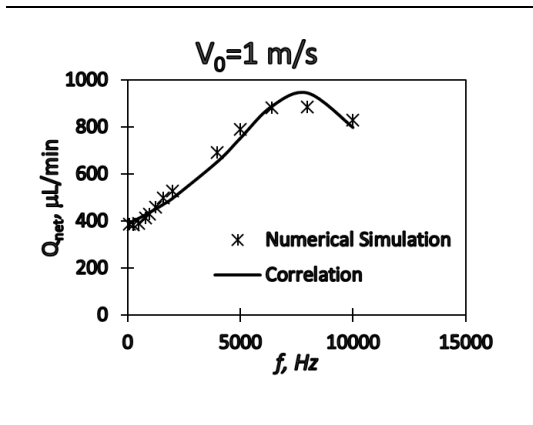
Figure 8 Comparison between Correlation and numerical simulation results at $V_0 = 1$ m/s

6.3 Peak velocity effect on resonance frequency

The resonance frequency is the optimum operating frequency. Therefore, the effect of peak velocity on the resonance frequency is important to be studied. Figure 9 shows that the resonance frequency is directly proportional to the applied peak velocity.
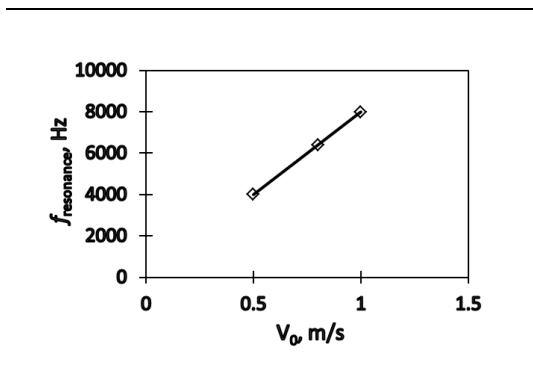

Figure 9 Effect of peak velocity on resonance frequency

6.4 Abrupt area ratio effect

The abrupt expansion/contraction element is the main element in the micro pump. It is the main cause of the rectification process. Figure 10 shows the effect of changing the area ratio of the abrupt expansion/contraction element on the

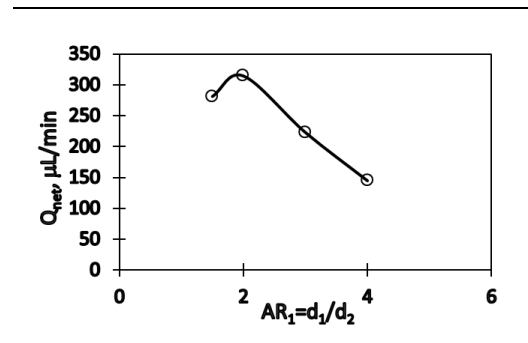net flow rate. This figure shows that the optimum abrupt area ratio is $AR_1 = 2$.

Figure 10 Effect of the abrupt area ratio change on the net flow rate

6.5 Diaphragm area ratio effect

The diaphragm size affects mainly the micro pump size. Therefore, it has a significant effect on its net flow rate as shown in Figure 11. The net flow rate increases with increasing diaphragm area ratio, as it directly increases the micro pump size.
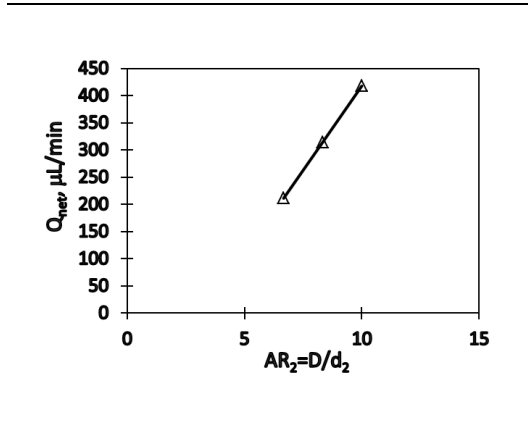

Figure 11 Effect of the diaphragm area ratio on the net flow rate

6.6 Pump size effect

The effect of increasing the whole micro pump size is presented in this section. There are three studied cases; the first case is the main case (normal case). The second case is the same main case, but scaled by a factor of 0.5 (Case 9). Whereas, the third case is scaled by a factor of 2 (Case 10).

Figure 12 shows the effect of operating frequency on the micro pump net flow rate for the three cases. The net flow rate increased with increasing pump size as expected. The interested result is that the optimum frequency i.e. resonance frequency changed for the three cases and follows relation (Error! Reference source not found.). As the optimum frequency of normal case is 4000 Hz, while for small size (Case 9) the optimum frequency is doubled to 8000 Hz as its mass decreased by one forth its value. Also, for large case (Case 10) the optimum frequency decreased to 2000 Hz (i.e. half of main case value), as its mass increased four times its original value. Singh et al. (2015) also reported that the natural frequency has a strong dependence on the mass within the system.

$$f_{resonance} \; \alpha \; \sqrt{\frac{1}{m}} \qquad\qquad (6)$$

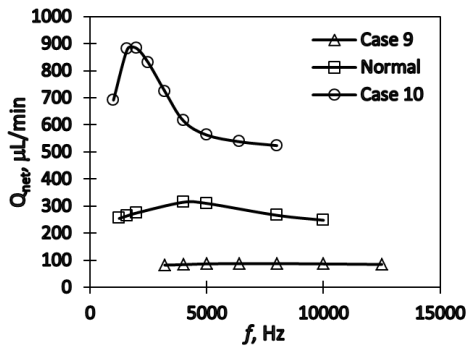where m is the mass of the system (kg).

Figure 12 Effect of operating frequency on net flow rate at various pump sizes

6.7   Fluid properties effect

To study the effect of fluid properties on pump performance, the listed cases in Table 4 and its corresponding net flow rate values are studied.

Table 4 Effect of fluid properties on pump performance

Case	μ (Pa.s)	P (kg/m^3)	ν=μ/ρ (m^2/s)	Q_{net} (μL/min)
Normal	0.001	998.2	1e-6	314.4
Case 11	0.004	998.2	4e-6	87.2
Case 12	0.004	800	5e-6	71.30
Case 13	0.002	1996.4	1e-6	314.4

The results show that the main affecting fluid property is its kinematic viscosity.

6.8   Performance characteristics

The micro pump performance was studied for the main case at the same applied peak velocity. In this section, the effect of applied back pressure on net flow rate is presented.

6.8.1   Effect of back pressure at different applied frequency values

The applied back pressure is inversely proportional to the net flow rate as shown in Figure 13. The same trend is also presented by Herz et al. (2008), as the net flow rate decreases with increasing the applied back pressure.
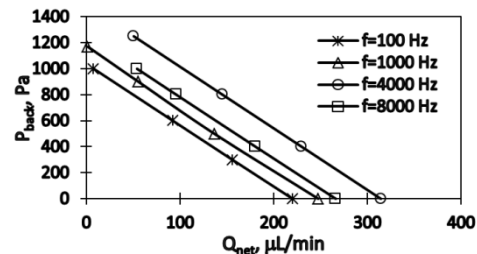

Figure 13 Back pressure effect on net flow rate at different operating frequencies

Also, results show that all lines have a linear trend and the same slope for all operating frequencies.

6.8.2 Effect of back pressure at different abrupt area ratio values

Figure 14 shows the effect of changing abrupt area ratio on the pump performance at different backpressure values.
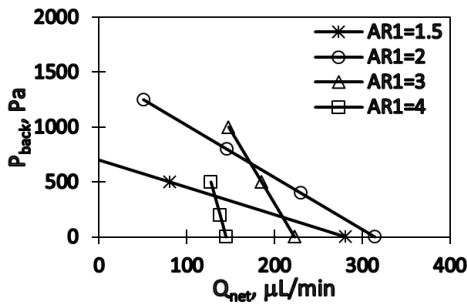

Figure 14 Effect of abrupt area ratio on micro pump performance

As mentioned before the maximum net flow rate is at $AR_1=2$, while, the micro pump maximum head (i.e. back pressure) is increased with increasing the abrupt area ratio. The slopes of all abrupt area ratio value lines are not the same. The slope increases with increasing the abrupt area ratio value.

6.8.3 Effect of back pressure at different diaphragm area ratio values

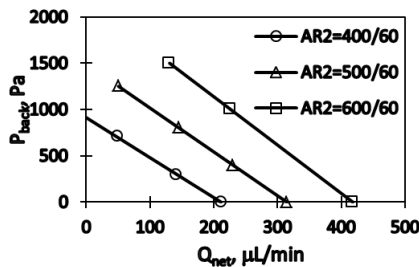Increasing diaphragm area ratio increases the whole micro pump performance, as shown in Figure 15.

Figure 15 Effect of diaphragm area ratio on micro pump performance

6.8.4 Principle of superposition

The effect of back pressure on net discharge can be studied using the principle of superposition. If we assume that back pressure effect is only to induce a flow in the opposite direction, which reduces thus net flow. Then, pump characteristics would be linear as has been observed. However, the slope of this line is different from that of flow induced by back pressure assuming steady flow as shown by Figure 16. The produced flow rate for steady case is superposed to that of the main case of zero back pressure. The net flow rate for the whole simulation case and superposition case are compared in Figure 16
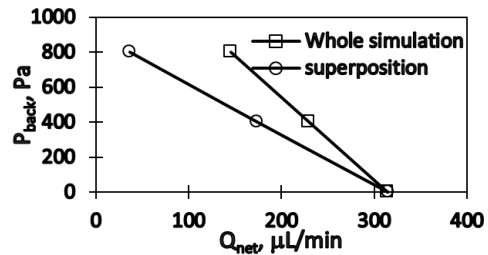

Figure 16 Superposition and simulation cases for pump performance

The figure shows that the net flow from whole simulation is larger than superposition case for constant back pressure. The main reason for that is the steady case (superposition) has lower energy losses due to the absence of moving wall of the diaphragm. Therefore, the flow rate for the steady case is higher than that of the whole simulation.

6.9 Correlations for micro pump performance

The dimensionless correlation for pump performance is given as the following for all simulated cases.

$$\dot{H} = A(1 - \dot{Q}) \qquad\qquad (7)$$

Where the dimensionless head ($\dot{H}$) and flow rate ($\dot{Q}$) are defined by equations (Error! Reference source not found.) & (Error! Reference source not found.), respectively.

$$\dot{H} = \frac{\Delta P}{\rho * V_0 * V_{largest}} \qquad (8)$$

$$\dot{Q} = \frac{Q_{net}}{Q_{net|p=0}} \qquad (9)$$

Where

$\dot{H}$	Dimensionless back pressure.
ΔP	Applied back pressure (pump head), Pa.
ρ	Fluid density, kg/m^3.
V_0	Applied peak velocity of the diaphragm, m/s.
$V_{largest}$	Velocity at P=0 Pa, related to the smallest diameter d$_2$, m/s.
$\dot{Q}$	Dimensionless net flow rate.
Q_{net}	Net flow rate, µL/min.
$Q_{net|p=0}$	Net flow rate at zero back pressure, µL/min.

The parameter (A) in equation (7) is related to the micro pump peak velocity and can be expressed by the following correlation:

$$A = 22.1 * e^{-0.531 * V_0} \qquad (10)$$

In addition, the flow rate at zero back pressure is given by equation (Error! Reference source not found.) and $V_{largest}$ is calculated by the following relation:

$$V_{largest} = \frac{Q_{net|p=0}\left(\frac{\mu L}{min}\right)}{1800} \qquad (11)$$

Figure 17 shows the correlation and numerical simulation for micro pump performance results.

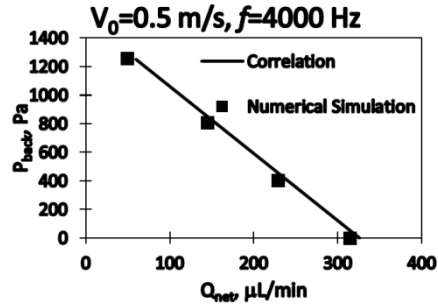*Figure 17 Pump performance at V$_0$=0.5 m/s and f=4000 Hz*

7   Nozzle/diffuser valve-less micro pump

The whole studied cases are for the abrupt contraction/expansion micro pump. So, the comparison between this type and the conventional nozzle/diffuser micro pump is important to be studied. The selected cases for the nozzle/diffuser micro pump are typical as the studied cases and just replace the abrupt element by nozzle/diffuser element as shown in Figure 18.

The abrupt area change is considered a special case of the nozzle/diffuser element having a half angle, α of 90$^\text{o}$. The changes of the net flow rate with the nozzle/diffuser angle is presented in Figure 19 for peak velocity V$_0$=0.5 m/s and operating frequency of f=2000 Hz.

This figure illustrates that the net flow rate increases with decreasing the tested angle α. Also, these results were presented by (Nabavi 2009). He concluded that the critical included angle is (10-20 degree). Moreover, it is found that the improvement due to this critical included angle is not above 6 %. So, the advantage of manufacturing simplicity of the abrupt element over the nozzle/diffuser element supersedes the small improvement in the net flow rate.

Figure 18 Nozzle/Diffuser micro pump

Figure 19 Net flow rate at various tested angles

This figure illustrates that the net flow rate increases with decreasing the tested angle α. Also, these results were presented by (Nabavi 2009). He concluded that the critical included angle is (10-20 degree). Moreover, it is found that the improvement due to this critical included angle is not above 6 %. So, the advantage of manufacturing simplicity of the abrupt element over the nozzle/diffuser element supersedes the small improvement in the net flow rate.
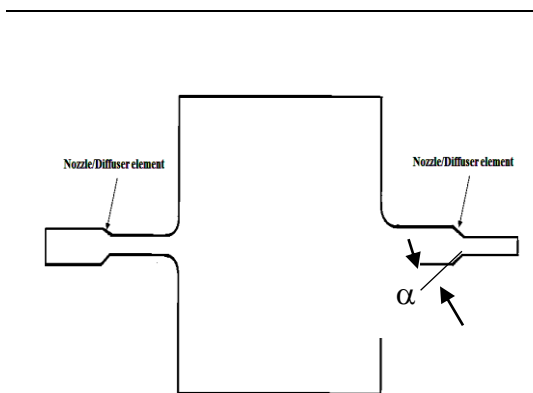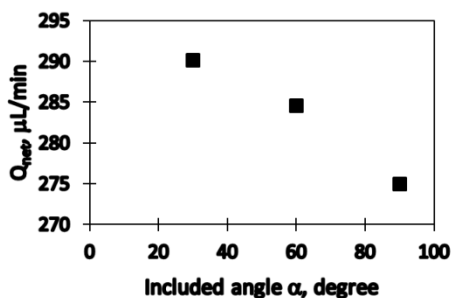
8 Conclusions

A two-dimensional numerical simulation has been performed for the valve-less micro pump incorporating abrupt expansion/contraction elements for rectification purpose rather than the conventional nozzle/diffuser elements. The

maximum Reynolds number based on the maximum velocity at smaller section of the outlet element is $Re_{max}=170$ and the flow is considered laminar. The effects of operating and design conditions, and fluid properties on the pump performance were introduced. The following conclusions are drawn:

- The net flow rate increases with frequency until the resonance frequency is reached. The net flow rate decreases with frequency for frequency values higher than that of the resonance value.
- The resonance frequency depends on the pump size (system mass), as it approximately equals the system natural frequency. Also, it depends on the applied peak velocity.
- The optimum area ratio for the abrupt expansion/contraction element is found to be $AR_1=2$.
- Fluid kinematic viscosity is the only fluid physical property that affects the net flow rate. Changing any other property (density or dynamic viscosity) while keeping the kinematic viscosity constant has no effect on the net flow rate.
- The performance characteristics of the micro pump (net flow as a function of back pressure) has a linear trend in all studied cases.
- Pump head increases with increasing abrupt area ratio value, while the net flow rate decreases.
- Increasing the diaphragm area ratio also increasing the whole micro pump performance (i.e. head and net flow rate).
- Correlations for dimensionless performance characteristics have been introduced, with an acceptable error, for a micro pump preliminary design. It mainly guides designers in understanding trends.
- The net flow rate for the studied type (abrupt changes) is lower than that for the conventional nozzle/diffuser micro

pump by 6%. Manufacturing simplicity of abrupt area change offsets the small advantage of the non-abrupt case.

Nomenclature
Roman Characters

A	Constant related to peak velocity
AR	Area ratio
C	Constant related to velocity ratio
$\acute{C}$	Constant related to pump net flow rate
d_1	Abrupt large section width, m
d_2	Abrupt small section width, m
D	Diaphragm width, m
f	Operating frequency, Hz
G	Gravitational acceleration, m/s^2
$\acute{H}$	Dimensionless micropump head
L	Abrupt sections length, m
L	Micropump chamber height, m
m	System mass, kg
N	Number of time steps per cycle
P	Pressure, Pa
Q	Flow rate, m^3/s
$\acute{Q}$	Dimensionless flow rate
T	Time, s
V	Velocity, m/s
x	Distance from diaphragm center, m

Greek Characters

α	Half angle of nozzle diffuser element, degree
ΔP	Applied pressure difference, Pa
Δt	Time step, s
ζ	Parameter related to peak velocity
μ	Dynamic viscosity, Pa.s
ν	Kinematic viscosity, m^2/s
ρ	Density, kg/m^3
τ	Time constant, s
$\acute{\tau}$	Time constant related to micro pump, s
ω	Angular frequency, rad/s

Subscripts

0	Reference value
1	Abrupt
2	Diaphragm
Back	Pump outlet
Backward	Contraction direction
Forward	Expansion direction
Largest	Corresponding to zero back pressure
Max	Maximum
Net	Net flow rate
$net\|p = 0$	Net flow at zero back pressure
O	Peak
Resonance	Optimum frequency

Acronyms

2D	Two dimensional
3D	Three dimensional
CFD	Computational Fluid Dynamics
PZT	Lead Zirconate Titanate
Re	Reynolds Number
UDF	User Defined Function

References
[1.] Abhari, F., Jaafar, H. and Md Yunus, N.A., 2012. A comprehensive study of micropumps technologies. *International Journal of Electrochemical Science*, 7(10), pp. 9765–9780.

[2.] Ahmadian, M.T. and Mehrabian, A., 2006. Design optimization by numerical characterization of fluid flow through the valveless diffuser micropumps. *Journal of Physics: Conference Series*, 34, pp. 379–384.

[3.] "ANSYS 15.0 Capabilities Brochure". Available:

http://www.ansys.com/Products/Simul
ation+Technology/Fluid+Dynamics/Fl
uid+Dynamics+Products/ANSYS+Flu
ent

[4.] Devarajan, R.,Mahendran, S., Abdul Karim, Z.A. and Nagarajan, T., 2011. Design of valveless micropump using preliminary characteristics from fluid flow. *Journal of Applied Sciences*, 11(11), pp. 2072–2075.

[5.] Fan, B., Song, G. and Hussain, F., 2005. Simulation of a piezoelectrically actuated valveless micropump. *Smart Materials and Structures*, 14(2), pp. 400–405.

[6.] Herz, M., Wackerle, M., Bucher, M., Horsch, D., Lass, J., Lang, M. and Richter, M., 2008. A Novel High Performance Micropump for Medical Applications. *ACTUAROR*, pp. 2–5.

[7.] Johari, J. and Majlis, B.Y., 2010. Design Simulations of MEMS Micropump by 3D Fluid-Structure Interaction Analysis. , 2, pp. 677–680.

[8.] Lan, W.P., Chang, J.S., Wu, K.C. and Shih, Y.C., 2008. Simulation of valveless micropump and mode analysis. , (April), pp. 25–27.

[9.] Li, S. and Chen, S., 2003. Analytical analysis of a circular PZT actuator for valveless micropumps. *Sensors and Actuators, A: Physical*, 104(2), pp. 151–161.

[10.] Nabavi, M., 2009. Steady and unsteady flow analysis in microdiffusers and micropumps: a critical review. *Microfluidics and Nanofluidics*, 7(5), pp. 599–619.

[11.] Nagy, Z., 2005. FEM simulation of microfluidic devices. , 3-week project demand. Available at: http://web-files.ait.dtu.dk/bruus/TMF/publications/3week/Jun2005membrane_pump.pdf.

[12.] Rabie, M. 2015 (to be published). Modeling and simulation of flow in a micropump. Master thesis, Faculty of Engineering Mansoura University.Ray,

S., Biswas, N. and Roy, P.C., 2012. Investigation of Newtonian Fluid Flow through a Two- dimensional Sudden Expansion and Sudden Contraction Flow Passage. *International Journal of Engineering Research and Development*, 1(12), pp.1–9.

[13.] Singh, S., Kumar, N., George, D. and Sen, A.K., 2015. Analytical modeling, simulations and experimental studies of a PZT actuated planar valveless PDMS micropump. *Sensors and Actuators A: Physical*, 225, pp. 81–94.

[14.] Singhal, V., Garimella, S. V. and Murthy, J.Y., 2004. Low Reynolds number flow through nozzle-diffuser elements in valveless micropumps. *Sensors and Actuators, A: Physical*, 113(2), pp. 226–235.

[15.] Yakhot, A., Arad, M. and Ben-Dor, G., 1999. Numerical investigation of a laminar pulsating flow in a rectangular duct. *International Journal for Numerical Methods in Fluids*, 29, pp. 935–950.

[16.] Yang, C.C., Miao, J.M., Lih, F.L., Liu, T.L. and Ho, M.H., 2011. The Performance Analysis of Valveless Micropump with Contoured Nozzle / Diffuser. *World Academy of Science, Engineering and Technology*, 5(2) , pp. 1011-1016.

[17.] Yang, H., Tsai, T.H. and Hu, C.C., 2008. Portable valve-less peristaltic micropump design and fabrication. *DTIP of MEMS and MOEMS - Symposium on Design, Test, Integration and Packaging of MEMS/MOEMS*, (April), pp. 273–278.